

Sudan Black B Pretreatment to Suppress Autofluorescence in Silk Fibroin Scaffolds

Olivia Foster,[†] Sawnaz Shaidani,[†] Sophia K. Theodossiou,[†] Thomas Falcucci, Derek Hiscox, Brooke M. Smiley, Chiara Romano, and David L. Kaplan*

Cite This: *ACS Biomater. Sci. Eng.* 2023, 9, 3193–3205

Read Online

ACCESS |

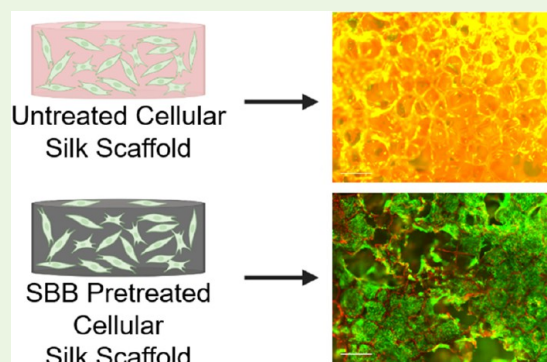
Metrics & More

Article Recommendations

Supporting Information

ABSTRACT: Natural polymers are extensively utilized as scaffold materials in tissue engineering and 3D disease modeling due to their general features of cytocompatibility, biodegradability, and ability to mimic the architecture and mechanical properties of the native tissue. A major limitation of many polymeric scaffolds is their autofluorescence under common imaging methods. This autofluorescence, a particular challenge with silk fibroin materials, can interfere with the visualization of fluorescently labeled cells and proteins grown on or in these scaffolds, limiting the assessment of outcomes. Here, Sudan Black B (SBB) was successfully used prefixation prior to cell seeding, in various silk matrices and 3D model systems to quench silk autofluorescence for live cell imaging. SBB was also trialed postfixation in silk hydrogels. We validated that multiple silk scaffolds pretreated with SBB (hexafluoro-2-propanol-silk scaffolds, salt-leached sponges, gel-spun catheters, and sponge-gel composite scaffolds) cultured with fibroblasts, adipose tissue, neural cells, and myoblasts demonstrated improved image resolution when compared to the nonpretreated scaffolds, while also maintaining normal cell behavior (attachment, growth, proliferation, differentiation). SBB pretreatment of silk scaffolds is an option for scaffold systems that require autofluorescence suppression.

KEYWORDS: Sudan Black B, silk fibroin, autofluorescence, DAPI, phalloidin, scaffolds, quenching stain



INTRODUCTION

Naturally derived biopolymers have been substantially used as scaffold materials in tissue engineering and three-dimensional (3D) disease modeling for various systems due to their cytocompatibility, biodegradability, and their ability to mimic the architectural and mechanical properties of many native tissues.¹ Understanding cellular interactions with these scaffolds is crucial for generating and understanding biomimetic tissue systems. Analytical techniques to study these cell–material interactions include viability assays, flow cytometry, Western blotting, scanning electron microscopy (SEM), and fluorescence labeling, among others.² Of these methods, fluorescence labeling allows the examination of cellular morphology and the spatial distribution of protein expression in polymeric scaffolds and is key for studying cell behavior. Polymeric scaffolds have enabled three-dimensional (3D) cell culture, expanding our understanding of cell behavior under conditions that better mimic the architecture of native tissue. However, a major limitation of many natural polymeric scaffolds is their autofluorescence under excitation signals typically used in fluorescence microscopy.^{2,3} Autofluorescence decreases the signal-to-noise ratio in the resulting images, making it challenging to differentiate between the scaffold material and fluorescently labeled cells and proteins.

Various treatments have been utilized to overcome the background autofluorescence of biomaterials to improve the resolution of fluorescent tagging of cells and proteins, including UV irradiation⁴ and dye staining to quench autofluorescence.⁵ Dyes such as Trypan Blue, Pontamine Sky Blue, Sudan Black B (SBB), and others have been used to eliminate background fluorescence in brain and other tissue sections to enable the evaluation of tissue composition and morphology via fluorescent labeling.^{4–9} SBB was effective in reducing background signaling and improving image resolution of fluorescent signaling in tissues but has not been used extensively to reduce autofluorescence in silk biomaterials.

Traditionally, SBB treatment was applied immediately following fixation or immunolabeling.^{4–9} Although SBB successfully suppressed autofluorescence and improved visualization of tissues, this postfixation treatment typically reduced the intensity of the fluorescently labeled targets, although the

Received: February 2, 2023

Accepted: April 10, 2023

Published: May 12, 2023



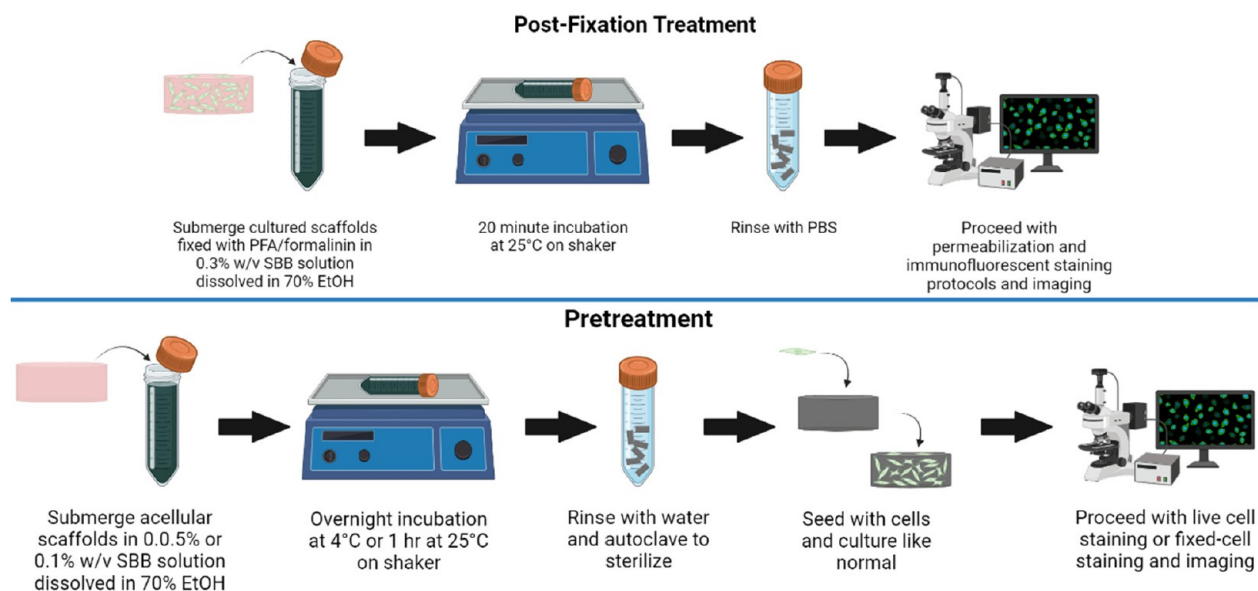


Figure 1. SBB postfixation treatment and pretreatment protocol on silk matrices to quench autofluorescence. Figure created with [BioRender.com](https://www.biorender.com).

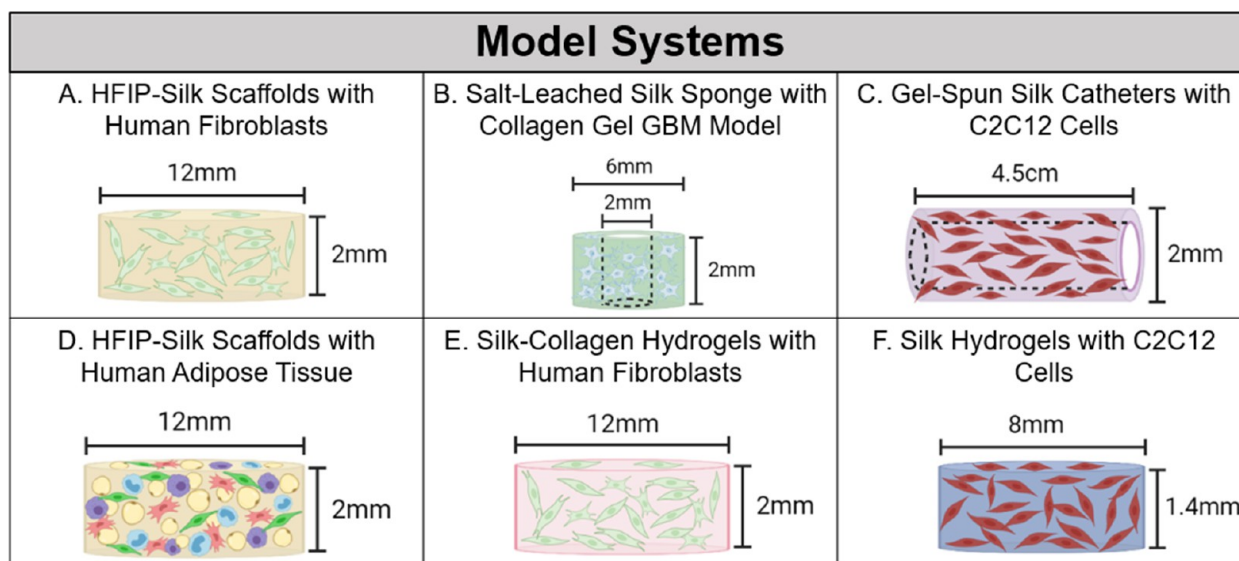


Figure 2. Silk protein-based model systems used to validate SBB postfixation treatment and pretreatment protocols. A: HFIP-silk scaffolds seeded with neonatal human dermal fibroblasts (NHDF) used to compare SBB postfixation treatment and pretreatment protocols. B: Salt-leached silk sponge + ECM glioblastoma (GBM) model seeded with human U87-MG cells used to compare SBB postfixation treatment and pretreatment protocols. C: Gel-spun silk catheters seeded with mouse C2C12 muscle cells used to compare SBB postfixation treatment and pretreatment protocols. D: HFIP-silk scaffolds seeded with primary human subcutaneous adipose tissue used to compare SBB postfixation treatment and pretreatment protocols. E: Silk-collagen hydrogels with incorporated NHDFs used to validate SBB postfixation treatment. F: Silk hydrogels with incorporated C2C12s used to validate SBB postfixation treatment. Figure created with [BioRender.com](https://www.biorender.com).

images obtained were better quality than those from control samples without SBB postfixation treatment.⁷ SBB postfixation treatment was also effective with cell-seeded polymer scaffolds as the last step in cytochemical analysis to improve cell visualization.¹⁰ Notably, poly(glycerol sebacate) (PGS), poly(urethane) (PU), poly(l-lactide-co- ϵ -caprolactone) (PLCL), and poly(lactic acid-coglycolic acid) (PLGA) all interacted differently with SBB. The authors attributed these differences to the dye interacting with hydrophobic regions of the polymers, both absorbing light emitted/scattered by the polymers and smoothing the surfaces to change refraction and light scattering properties.¹⁰

Silk-based biomaterials have been successfully utilized as scaffold materials in tissue engineering and 3D disease modeling for brain, intestine, and skin,^{11–13} among other tissues. However, the autofluorescence of silk is a limiting factor in its use in cell culture and tissue engineering applications where extensive quantification of cell morphology or protein localization are needed. The efficacy of SBB staining to suppress autofluorescence of silk electrospun mats seeded with cells has been previously demonstrated, but only as a postfixation treatment.¹⁴ In prior studies, SBB staining was conducted immediately postcell fixation or postimmunostaining (Figure 1). Overall, the SBB staining quenched endogenous fluorescence of the silk-based biomaterials while

maintaining satisfactory image resolution of cells and proteins fluorescently tagged on the scaffolds. However, despite some prior success in using SBB, SBB treatment postfixation can reduce fluorescent tag intensity and may also disrupt intercellular structures, particularly in nonelectrospun silk-based scaffolds used more frequently in soft tissue engineering applications.² SBB remains underexplored in hydrogel and hydrogel-sponge composite systems, which are commonly used as tissue engineering support materials.¹⁵ Moreover, SBB is known to reduce into carcinogenic and genotoxic metabolites in the human gastrointestinal tract and in vitro studies¹⁶ and is only soluble in solvents that are harmful to cells, a major limitation for applications with live cell imaging. This limitation was partially addressed by prior studies using SBB pretreatment after polycaprolactone (PCL) scaffold fabrication and prior to cell seeding, where autofluorescence was suppressed to enable live cell viability and imaging for up to 28 days in culture.² The success of SBB as a pretreatment for PCL scaffolds suggested that this approach may be effective for the pretreatment of silk biomaterials. Taken together, there is a significant need to develop additional methods for utilizing SBB staining as both a pre- and postfixation treatment to suppress the autofluorescence of silk-based biomaterials.

In the present study, we developed a series of reproducible material preparation and staining methods for the application of the SBB pretreatment (Figure 1) with various silk protein scaffolds seeded with different cell types (Figure 2). The various methods were designed to suppress silk autofluorescence and improve resolution of both fluorescently labeled fixed cells and live cell images. Endogenous fluorescence suppression was evaluated by culturing fibroblasts, myoblasts, and neural cells on multiple formats of 3D silk scaffolds. Suppression of autofluorescence was studied for up to 28 days. Mechanical properties were examined to ensure SBB pretreatment did not compromise the material properties of the scaffolds. The results indicated that SBB pretreatment of silk scaffolds suppressed autofluorescence and was readily combined with multiple protocols that are compatible with both live and fixed cell imaging, while maintaining normal cell behavior and scaffold properties.

METHODS

Silk Degumming and Dissolution. All silk materials used in this study were initially prepared via degumming and dissolution of silk as previously reported.¹⁷ Briefly, 5 g of *Bombyx mori* cocoons were cut and degummed by boiling at 100 °C in 0.02 M sodium carbonate solution for 30 or 60 min, to remove the sericin (silkworm silk is composed of two main proteins, fibroin and sericin). After washing and drying, the silk fibroin (hereafter referred to as silk in this work) was dissolved in aqueous 9.3 M lithium bromide solution for 4 h at 60 °C to yield a 20% weight-by-volume (w/v) solution. The solution was then dialyzed against distilled water for 3 days with 2–3 washes per day and centrifuged at 9,000 rpm for 20 min at 4 °C twice to remove any silk aggregates. The silk was then concentrated to at least 6% (w/v) using Slide-a-Lyzer dialysis cassettes and Pierce dialysis membranes, with a molecular weight cutoff 3500 Da (Thermo Scientific, Waltham, MA).

Preparation of Hexafluoro-2-propanol (HFIP)-Silk Scaffolds. HFIP-silk scaffolds were prepared as previously described.^{18,19} Briefly, lyophilized silk solution was dissolved in HFIP (Fisher, Waltham, MA) to obtain a 17% (w/v) HFIP-silk solution. Then 2 mL of the HFIP-silk solution was poured over 6.8 g of sodium chloride (NaCl) (Sigma-Aldrich, St. Louis, MO), sieved to 500–600 μ m size, in a glass scintillation vial for 24 h and sealed. After 24 h, the seal was opened, and excess HFIP was allowed to evaporate for 24 h in a fume hood.

Methanol (MeOH) (Fisher) was poured into the glass containers and sealed for 24 h, and then the seal was opened to allow methanol to evaporate for another 24 h. Glass vials were placed in a 2L beaker of DI water for 3 days to wash out the salt, changing the water two to three times per day. The silk scaffolds were then cut to size (2 mm height \times 12 mm diameter cylinders) using a 12 mm biopsy punch and scalpel, autoclaved in water using a liquid cycle before use, and stored in sterile distilled water until used.

Preparation of Glioblastoma (GBM) Salt-Leached Silk Sponge Scaffolds. The salt-leached silk sponge scaffolds were formulated as previously described.^{11,20} NaCl was sieved to separate the 500–600 μ m diameter granules. Then 30 mL of 6% (w/v) silk solution was poured into a 100 mm Petri dish, and 60 g of sieved NaCl was carefully and uniformly poured on the silk solution. The Petri dish was incubated for 48 h at room temperature to allow the salt to induce the physical cross-linking of the silk. The Petri dish containing the scaffold was placed in a 60 °C oven without the lid for 1 h to evaporate any remaining liquid and then placed in a beaker containing 2L of distilled water for 4 days to wash the remaining salt out of the sponge, with 2–3 water changes per day. A 6 mm biopsy punch was used to cut the sponge to create scaffolds that fit in 96-well plates, and the center of each scaffold was cut out using a 2 mm biopsy punch. The scaffolds were then cut using surgical scissors to create “donut” scaffolds that were 2 mm in height. The miniature sponges were then immersed in distilled water, autoclaved, and stored at 4 °C in sterile distilled water until use.

Preparation of Silk-Collagen Hydrogels. Silk-collagen hydrogels containing 2.5% (w/v) of silk and 1 mg/mL of collagen were prepared as previously described.²¹ Briefly, 3.56 mL of 10 \times Minimum Essential Media (EMEM, Sigma), 0.325 mL of 100 \times Glutamax (Gibco, Waltham, MA), and 4.04 mL of fetal bovine serum (FBS) (Gibco) were combined. This solution was then further combined with 15 mL of silk solution (60 min extract, 7 wt %) and 15 mL of collagen (3 mg/mL, TeloCol-3 Bovine Collagen, Advanced Biomatrix, Carlsbad, CA). The mixture was neutralized with 1.12 mL of a 7.5% sodium bicarbonate solution. Then 0.15 mL of the enzyme HRP (Sigma-Aldrich) at a concentration of 1 U/mL was added to the solution, and then 1.65 mL of human fibroblasts was incorporated into the mixture for a final concentration of 500,000 cells/mL. Finally, 0.15 mL of the cross-linking agent H₂O₂ (Sigma-Aldrich) at 1% (w/v) was added, and the whole solution was mixed thoroughly. The solution was immediately transferred to transwell plates (Corning) and allowed to incubate 1 h at 37 °C and 5% CO₂ to fully gel before cell culture media was added below and on top of the gels.

Preparation of Silk Hydrogels. Silk hydrogels containing 2% and 4% w/v silk solution (the range used for most cell culture applications) were prepared as previously described.¹⁵ Briefly, silk solution was combined with 1 \times Dulbecco's Modified Eagle Medium (DMEM) (Gibco) to achieve the targeted silk concentration. Type IV horseradish peroxidase (HRP) (Sigma-Aldrich) and hydrogen peroxide (H₂O₂) (Sigma-Aldrich) were sterile-filtered and used to cross-link the hydrogels. HRP and H₂O₂ were used at concentrations of 10 U/mL and 0.01% w/v, respectively, resulting in gelation of the materials within 30 min in a 37 °C incubator. Acellular and cellular gels were prepared identically; however, for the cellular gels, cells were suspended within the DMEM solution prior to mixing with the aqueous silk solution.

Preparation of Silk Gel-Spun Catheters. Silk catheters were gel-spun according to previously established protocols,²² with unique specifications set for this study. Briefly, concentrated silk solution was mixed with 5% (w/v) poly(ethylene oxide) (PEO) (900,000 MW, Sigma-Aldrich) in an 80:20 silk:PEO volumetric ratio, to increase the final porosity of catheters. The solution was left at 4 °C for 1 h to allow for bubbles to escape. The Silk-PEO solution was then extruded via a syringe pump at 50 μ L/min from a 3 mL syringe through a 27-gauge, 0.5 in. (1.27 cm) blunt needle onto an axially reciprocating and rotating 1 mm diameter Teflon-coated mandrel. Catheters were immediately transferred from the gel-spinning device to an insulated box filled with dry ice. The catheters were left in the box for at least 30 min until they were completely frozen. Frozen catheters were

immediately lyophilized for 24 h using a Labconco FreeZone Lyophilizer (Labconco, Kansas City, MO). Following lyophilization, the catheters were soaked in 100% MeOH (Fisher) for 10 min to complete the physical cross-linking of the silk. Catheters were then soaked for 3 days in deionized (DI) water to remove any PEO and MeOH from the material. The water was changed once after the first day. Following fabrication, catheters were autoclaved and stored in sterile DI water until use.

SBB Pretreatment of Silk Scaffolds. After the salt-leached sponges and HFIP-silk scaffolds were prepared, samples of each material were treated with SBB (Sigma). SBB concentrations of 0.05%, 0.1%, and 0.3% (w/v) were prepared by dissolving SBB powder in 70% ethanol (EtOH) (Sigma). The scaffolds were immersed in various concentrations of SBB overnight with shaking at 4 °C. The scaffolds were then rinsed with DI water 4–6 times to remove unbound SBB and ethanol, reautoclaved, and rinsed with sterile distilled water (Sigma) and media (Gibco) to prepare for cell culture. HFIP-silk scaffolds made with SBB during fabrication were prepared by dissolving SBB in HFIP at 0.3% (w/v) before being used to dissolve the lyophilized silk.

SBB Pretreatment of Catheters. Following fabrication, catheters were submerged in a solution of 0.3% SBB in 70% EtOH for 60 min on a rocker at room temperature (25 °C). Catheters were then washed in sterile PBS six times for 30 min and stored in sterile PBS at 4 °C until used for cell culture.

SBB Post-Fixation Treatment of Scaffolds and Hydrogels. Postfixation SBB treatment was performed on HFIP-silk scaffolds, salt-leached silk scaffolds, and collagen-gel composite systems, silk-collagen hydrogels, silk-gels, and silk gel-spun catheters. After fixation of the scaffolds and hydrogels, they were submerged in a solution of 0.3% SBB for 20 min on a rocker at room temperature (25 °C) and were flipped halfway through the process. Scaffolds and hydrogels were then rinsed with PBS three times for 5 min each and used for subsequent immunofluorescence staining.

Human Dermal Fibroblast Culture in HFIP-Silk Scaffolds and Silk-Collagen Hydrogels. Neonatal human dermal fibroblasts (NHDF, #CC2509) (Lonza, Basel, Switzerland) were cultured in DMEM/F12 (Thermo Scientific) supplemented with 10% fetal bovine serum (FBS) (Gibco) and 1% antibiotic-antimycotic acid (Gibco). HFIP-silk scaffolds were coated with 0.1 mg/mL poly-D-lysine (Sigma-Aldrich) for 2 h at 37 °C or overnight at 4 °C. Scaffolds were washed with PBS three times and incubated with media for at least 30 min at 37 °C to equilibrate the scaffolds prior to seeding. NHDF were trypsinized (Gibco) and prepared in a 1×10^6 cells/mL solution. Then 0.5 mL of the cell solution was added to each scaffold (500,000 cells per scaffold) in 24-well plates and placed in a 37 °C and 5% CO₂ incubator. Media was changed every other day. For the silk-collagen hydrogels, NHDF was trypsinized and prepared in a 1.3×10^7 cells/mL solution and combined into the gel mixture during fabrication.

Adipose Tissue Culture. Adipose tissue scaffolds were prepared and cultured as previously described.¹⁸ Primary human subcutaneous adipose tissue was obtained from surgical procedures with institutional review board approval (Study00001914) from the National Disease Research Interchange (NDRI, Philadelphia, PA, USA). Briefly, HFIP-silk scaffolds were prepared by coating with 0.1 mg/mL poly-D-lysine for 2 h at 37 °C or overnight at 4 °C. Scaffolds were washed with PBS three times and incubated with media for 2 h at 37 °C. Adipose tissue was liquified in a blender, and prewarmed scaffolds were submerged in liquified adipose tissue in a 50 mL conical tube and placed in a 37 °C and 5% CO₂ incubator for 30 min. After 30 min, scaffolds were placed into individual wells of a 24-well plate and placed in the incubator for 2 h. The scaffolds were covered with DMEM/F12 (Thermo Scientific) supplemented with 10% FBS (Gibco) and 1% antibiotic-antimycotic (Gibco), and media was changed every other day.

Human Glioblastoma Cell Culture in Salt-Leached Scaffold. U87-MG (ATCC HTB-14, Manassas, VA) glioblastoma (GBM) cells were cultured in DMEM/F12 supplemented with 10% FBS (Gibco) and 1% antibiotic-antimycotic acid (Sigma-Aldrich). The bioengi-

neered GBM tissue culture system was set up as previously described.²⁰ Scaffolds were coated with 0.1 mg/mL poly-D-lysine (Thermo Scientific) for 2 h at 37 °C or overnight at 4 °C. Scaffolds were washed with PBS three times and incubated with media for at least 30 min at 37 °C to equilibrate the scaffolds prior to seeding. 100 μ L of U87-MG cell suspension (1×10^6 cells/mL, or 100,000 cells per scaffold) was added to each scaffold in 96-well plates and incubated overnight. The next day, the media was aspirated from all wells to remove nonadherent cells, and 3 mg/mL rat tail collagen type I (Corning) hydrogel solution was added to each scaffold for 30 min at 37 °C, as previously described.²³ Media was added to the wells, and the scaffolds were left to incubate overnight. The following day, scaffolds were carefully transferred to 24-well plates to undergo 7- or 28-day culture with appropriate media changes.

C2C12 Culture in Silk Hydrogels and on Gel-Spun Silk Catheters. C2C12 mouse myoblasts (ATCC #CRL-1772) were cultured on tissue-culture treated flasks according to established protocols.²⁴ Briefly, cells were grown in DMEM + Glutamax (Thermo Scientific) supplemented with 10% FBS (Gibco) and 1% antibiotic/antimycotic (Sigma-Aldrich) and grown to \sim 70% confluency. Myoblasts were used between passages 5 and 16. For experiments, cells were detached using 0.25% Trypsin-EDTA (Gibco) and seeded onto catheters directly or suspended in DMEM and mixed with an aqueous silk solution during hydrogel fabrication.

Live/Dead Staining. Scaffolds were removed from the culture at various time points, and viability was visualized via a LIVE/DEAD Viability/Cytotoxicity Kit (Invitrogen, Waltham, MA) according to the manufacturer's instructions. Scaffolds were incubated in a solution of 4 μ M ethidium homodimer-1 (EthD-1, dead stain) and 2 μ M Calcein AM (live stain) in D-PBS for 20–30 min at room temperature (RT). Images were taken with a Keyence All-in-One Fluorescent Microscope (BZ-X710, Keyence Corp, Osaka, Japan) with 4 \times , 10 \times , and 20 \times air objectives.

Viability Assay. Cell proliferation assays were performed for each time point via the water-soluble tetrazolium salt (WST-1) assay (Sigma-Aldrich) according to the manufacturer's instructions. Samples were incubated for 1 h at 37 °C in WST-1 solution diluted 1:10 in culture medium, including a media control. Absorbance was read at 450 and 600 nm on a H1 synergy microplate reader (BioTek Instruments, Winooski, VT, USA).

Immunostaining. Scaffolds were fixed at various time points using 4% paraformaldehyde (PFA) (Thermo Scientific) solution in PBS for 3 h at RT. Samples were washed three times with PBS (5 min per wash), permeabilized with 1% Triton X-100 (v/v%) (Sigma-Aldrich) in PBS for 10 min at room temperature, and rinsed with 0.1% Tween-20 (v/v%) (Sigma-Aldrich) in PBS (PBST) three times (5 min per wash). Samples were blocked with 1 \times blocking buffer (Abcam) for 30 min at RT. Primary antibodies (vimentin or phalloidin, already conjugated) were incubated overnight at 4 °C followed by PBST rinses (5 min, 3 times). Samples were incubated in Hoechst/DAPI (Invitrogen) for 20 min followed by PBS rinses (5 min, 3 times). Samples were stored in PBS and protected from light until viewing and imaged by using a Keyence fluorescence microscope (Keyence Corp).

Quantification of Immunofluorescence Staining. Immunofluorescent (IF) images of HFIP-silk scaffolds seeded with NHDF were analyzed using ImageJ to measure the intensity and area percentage. Each replicate was imaged in triplicate, and the green and blue channels were analyzed separately. The threshold function in ImageJ was used to select fluorescent areas of each image, and they were measured for intensity and percentage of area of the total image. The average intensity and area percentage were calculated from the triplicate images of each replicate, and replicates were averaged for each independent experiment. 2–4 independent experiments were conducted.

Characterization of Scaffold Morphology. Scaffold morphology was determined via scanning electron microscopy (SEM) using a Zeiss Supra55VP SEM (Carl Zeiss, Heidenheim, Germany). After preparation of untreated, 0.05%, 0.1%, and 0.3% SBB treated scaffolds, they were air-dried for 8 h. Dried samples were placed in carbon

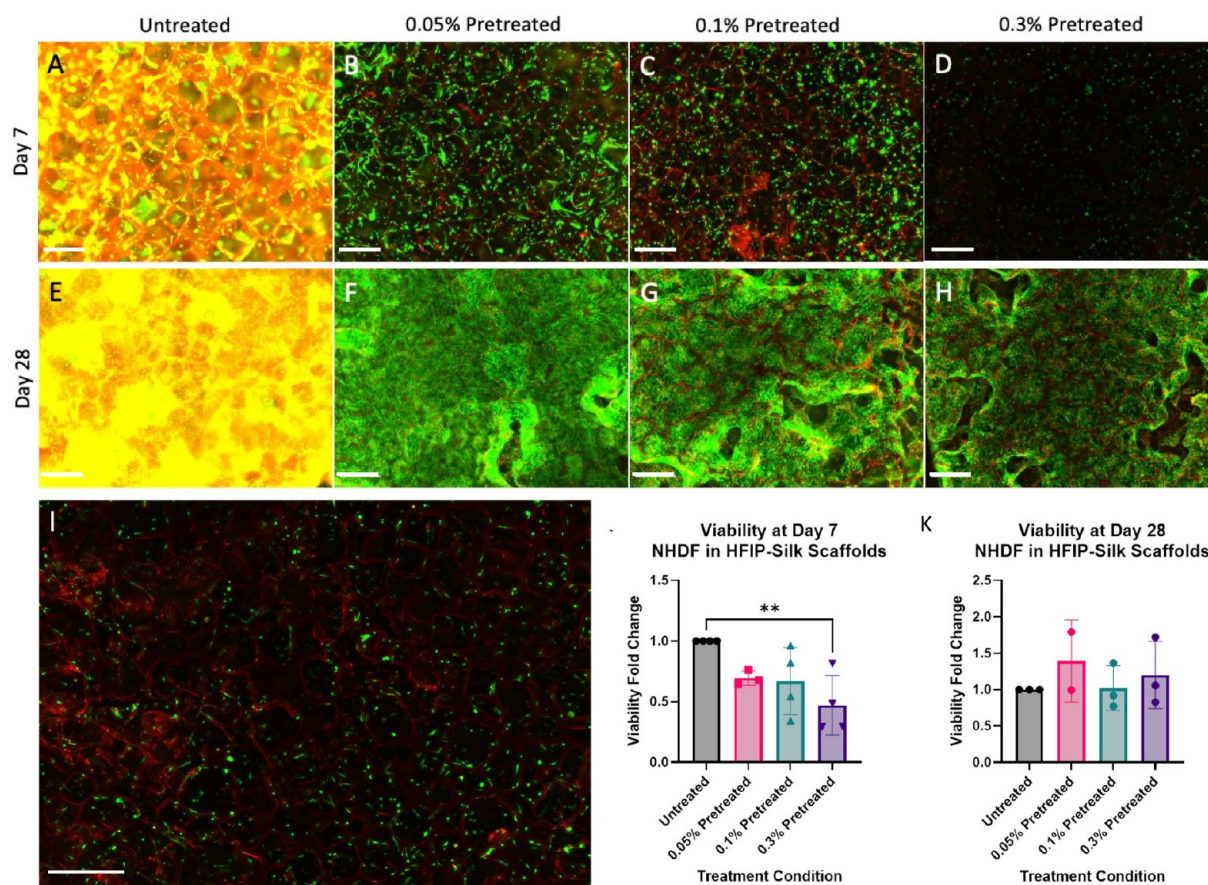


Figure 3. Live/dead staining of NHDF in HFIP-silk scaffolds. Green (Calcein AM) indicates live cells and red (ethidium homodimer-1) stain indicates dead cells. A–D: Day 7 of culture. E–H: Day 28 of culture. Left to right: untreated, 0.5% SBB pretreated, 0.1% SBB pretreated, 0.3% SBB pretreated. Scale bar = 500 μm . I: Live/dead stain of NHDF in HFIP-silk scaffolds at day 7 of culture. These scaffolds were fabricated by dissolving SBB in the HFIP at 0.3% (w/v). J,K: Viability of NHDFs in HFIP-silk scaffolds using a WST-1 assay at 7 and 28 days in culture. Error bars represent standard deviation. Each distinct experiment contained 1–2 scaffold replicates, with 2–4 distinct experiments for each treatment condition ($N = 2–4$). The average of these scaffold replicates per experiment represents each dot (ANOVA with Dunnett’s multiple comparison test, $**p = 0.0075$).

adhesive discs on SEM stubs and sputter coated with a thin layer of gold.

Mechanical Analysis. Scaffolds and gels were taken from culture at various time points. Unconstrained compression was performed by using a TA Instruments RSA3 Dynamic Mechanical Analyzer (TA Instruments, New Castle, DE). Samples were analyzed by inducing strain up to 30% of the initial height of each sample to account for the size disparity between samples. Catheters were mechanically evaluated in tension on an Instron device fitted with a 10 N capacity load cell (Instron Corp., White Plains, NY). Initial catheter lengths and widths were measured using calipers, and the cross-sectional area was estimated from scanning electron microscopy (SEM) images of the catheters. Catheters were preloaded to 0.1N to remove any slack and pulled to failure at a rate of 5 mm/min. These values were chosen based upon prior work.²² Stress–strain curves from each sample were analyzed to calculate the elastic modulus, ultimate tensile strength, and percent elongation upon failure (see [Supporting Information](#)).

Fourier Transform Infrared (FT-IR) Spectroscopy. Protein secondary structural analysis of the untreated, 0.05%, 0.1%, and 0.3% SBB treated scaffolds was carried out using a JASCO FTIR 6200 spectrometer (JASCO, Tokyo, Japan) with a MIRacle attenuated total reflectance (ATR) with a germanium crystal. FT-IR measurements were done using 64 scans, a resolution of 4 cm^{-1} within wavenumbers of 600–4000 cm^{-1} . Data analysis and percentage β -sheet content were performed and calculated as the ratio of the areas of peak absorbances at 1616–1621, 1622–1627, 1628–1637, and

1697–1703 cm^{-1} to the total area between 1580 and 1720 cm^{-1} as previously described (see [Supporting Information](#)).¹⁵

Statistical Analysis. All data are expressed as the mean \pm standard deviation. GraphPad Prism (GraphPad Software, La Jolla, CA) was used to perform one-way analysis of variance (ANOVA) with Dunnett’s multiple comparison test to determine statistical significance for most purposes unless otherwise stated. Treated scaffolds were compared to untreated scaffolds. Viability data were normalized against the untreated controls to compare the treated and untreated scaffolds.

RESULTS

HFIP-Silk Scaffolds. SBB Pretreatment Successfully Quenched Autofluorescence of Silk Sponges in Live Cell Imaging. SBB pretreatment was evaluated with the HFIP-silk scaffolds seeded with NHDF, and scaffolds pretreated with 0.05%, 0.1%, and 0.3% (w/v) solution of SBB successfully quenched autofluorescence based on live/dead imaging of NHDF in the HFIP-silk scaffolds ([Figure 3](#)). All images were taken at the same exposure, and the untreated scaffolds (controls) showed high levels of autofluorescence that led to low resolution images, particularly with the red channel (594 nm wavelength). All conditions of SBB pretreatment eliminated the majority of autofluorescence, leading to clearer visualization of individual cells. The 0.3% SBB pretreated

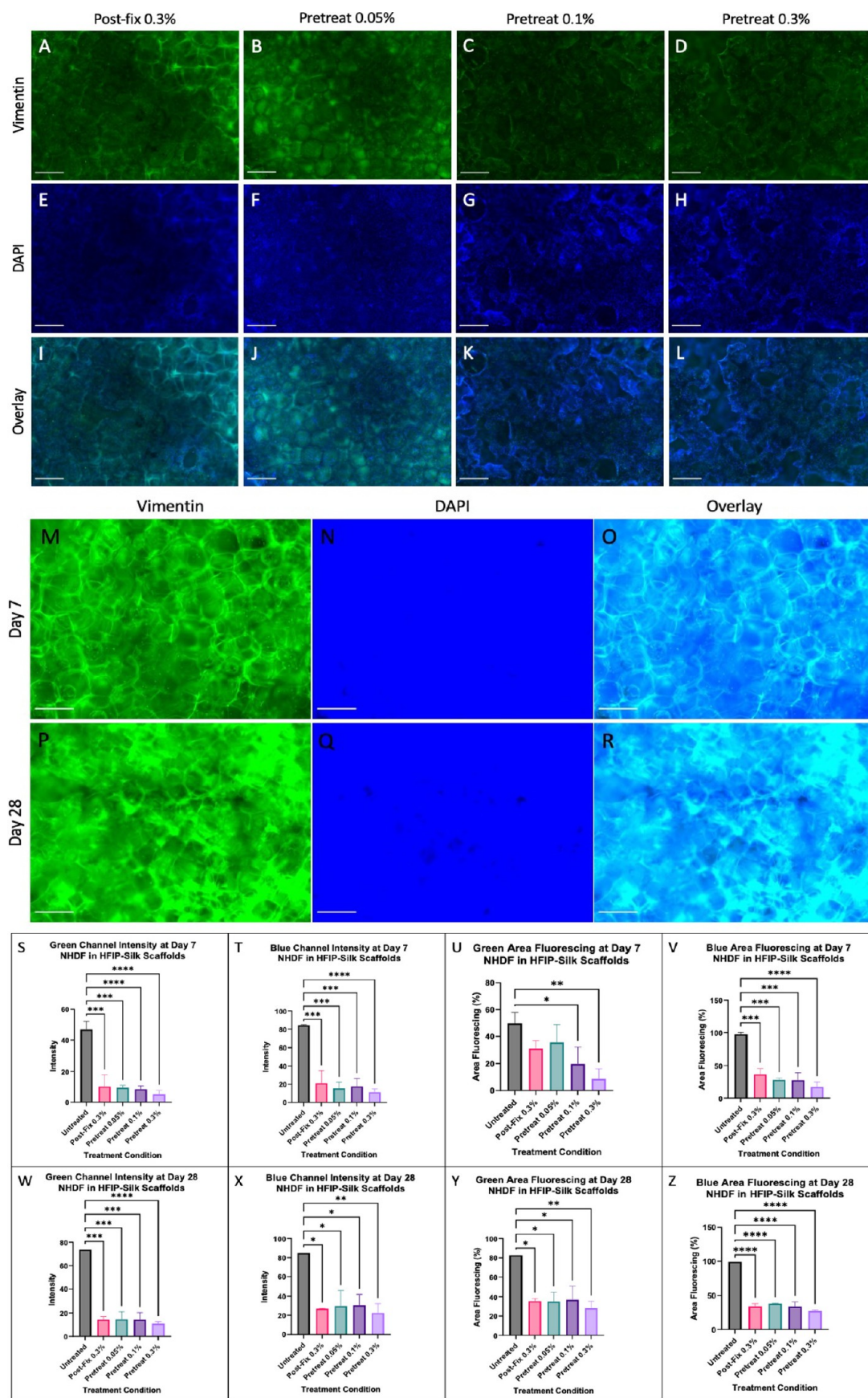


Figure 4. Immunofluorescence staining of NHDF in HFIP-silk scaffolds after 28 days of culture. A–D: Green channel for Vimentin 488 nm. E–H: Blue channel for DAPI 405 nm. I–L: Green and blue channel overlay. Left to right: 0.3% SBB postfixation treated scaffold, 0.05% SBB pretreated scaffold, 0.1% SBB pretreated scaffold, 0.3% SBB pretreated scaffold. M–R: Immunofluorescence staining of NHDF in untreated HFIP-silk

Figure 4. continued

scaffolds after 7 and 28 days of culture. M,P: Green channel images for Vimentin 488 nm. N,Q: Blue channel images for DAPI 405 nm. O,R: Green and blue channel overlay. Scale bar = 500 μm . S–Z: Quantification of immunofluorescence of NHDFs in HFIP-scaffolds. Images were quantified using ImageJ. Triplicate images of each scaffold replicate were averaged, and then scaffold replicates were averaged for each distinct experiment. Each experiment had 1–2 scaffold replicates, with 1–3 distinct experiments per condition ($N = 1$ –2 for untreated condition, $N = 2$ –3 for treated conditions). * = $p < 0.05$, ** = $p < 0.01$, *** = $p < 0.001$. **** = $p < 0.0001$, ANOVA and Dunnett's multiple comparison test.

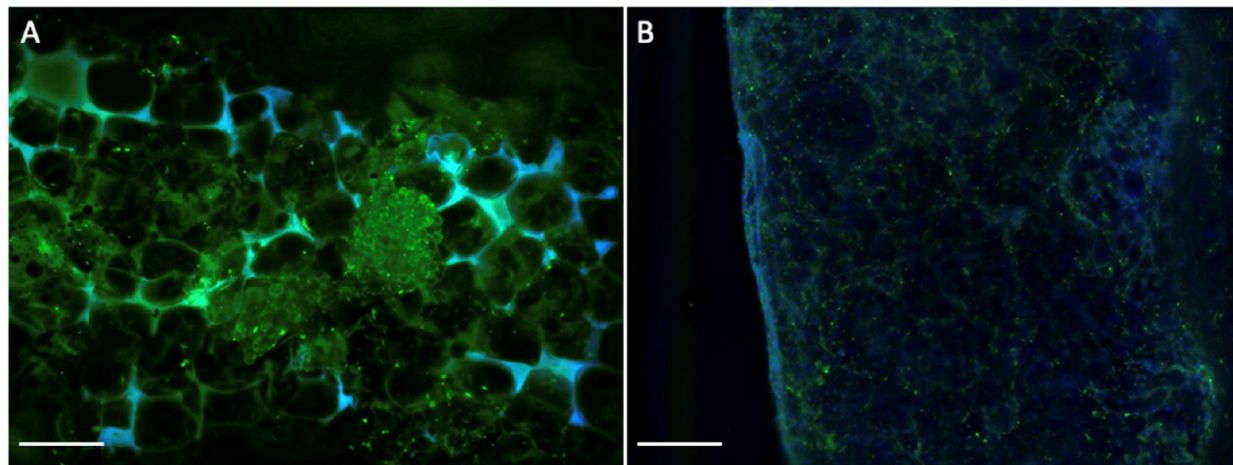


Figure 5. Immunofluorescence staining of adipose tissue in HFIP-silk scaffolds after 28 days of culture. A: 0.3% SBB postfixation treated scaffold. B: 0.1% SBB pretreated scaffold. Green channel for Vimentin 488 nm. Blue channel for DAPI 405 nm. Scale bar = 500 μm .

conditions demonstrated fewer live cells, with rounded cell morphology compared to the elongated fibroblasts in the 0.05% and 0.1% SBB pretreated conditions, indicating that pretreatment may negatively affect cell attachment and/or viability at the higher concentrations. The 0.05% and 0.1% SBB pretreatments were the most promising due to the suppression of autofluorescence and lack of negative impact on the cells by live/dead staining. The 0.3% pretreatment was used as a negative control after observing the decreased cell viability.

SBB as a pretreatment was also trialed during earlier stages of HFIP-silk scaffold preparation; scaffolds that were prepared using SBB dissolved in HFIP had fewer live cells and more dead cells than other conditions after 7 days of culture with NHDF cells (Figure 3), suggesting that SBB dissolved in HFIP might prevent cell attachment or negatively affect cell viability. Therefore, SBB dissolved in HFIP was not pursued for more than 7 days.

SBB Staining Did Not Significantly Affect Cell Viability at Lower Concentrations. WST-1 cell proliferation and viability assays were performed on the HFIP-silk scaffolds cultured with NHDF after 7 and 28 days in culture to investigate the SBB pretreatment effect on cell growth (Figure 3). The assays were performed on untreated, 0.05%, 0.1%, and 0.3% SBB pretreated scaffolds to determine if viability was concentration dependent. After 7 days in culture, the untreated condition had significantly higher cell viability than the 0.3% SBB pretreated condition (Figure 3A; $p = 0.0075$). The viability of the cells cultured in the 0.05% or 0.1% SBB pretreated conditions after 7 days was somewhat lower than that of the untreated control, but the difference was not significant (Figure 3B; $p = 0.1560$ and $p = 0.0864$, respectively). After 28 days in culture, viability did not differ significantly between treatment conditions, compared to the untreated controls ($p > 0.05$).

SBB Pretreatment Successfully Quenched Autofluorescence of HFIP-Silk Scaffolds in Fixed Cell Imaging. SBB

pretreatment more effectively suppressed autofluorescence of the silk scaffolds compared to the postfixation SBB treatment at day 7 (SI Figure 1) and day 28 (Figure 3) in culture. SBB pretreatment improved the resolution and contrast of cell markers without decreasing the fluorescence intensity of the antibody staining of the cells. The 0.1% and 0.3% SBB pretreatment conditions demonstrated less autofluorescence than the 0.05% SBB pretreatment or the 0.3% SBB postfixation conditions. All treatment conditions exhibited less intensity and fewer fluorescent areas compared to untreated conditions imaged at the same exposure levels (Figure 4).

SBB pretreatment and postfixation treatment demonstrated decreased intensity and area of fluorescence for the green (488 nm) and blue (405 nm) channels at days 7 and 28 compared to untreated control scaffolds (Figure 4). For the green channel areas of fluorescence on day 7, 0.1% and 0.3% SBB pretreated conditions were significantly lower than the untreated condition ($p = 0.0373$ and $p = 0.0081$, respectively), although all other treatment conditions also saw decreased intensity from the untreated condition ($p > 0.05$). For all other measurements, all treatment conditions (pretreatment and postfixation treatment) were significantly lower than the untreated condition for fluorescence intensity and area fluorescing (ANOVA, $p < 0.05$). The 0.1% and 0.3% SBB pretreatments had lower intensity and fluorescence area than 0.05% SBB pretreatment and 0.3% SBB postfixation treatment, corresponding to the improved image resolution and contrast seen for those conditions. The intensity and area of fluorescence of the green and blue channels at days 7 and 28 were not significantly different between the 0.3% SBB postfixation treatment and any of the pretreatment conditions, corresponding to the visual observations that SBB pretreatment did not diminish antibody fluorescent signaling intensity.

SBB Pretreatment Successfully Quenched Autofluorescence of HFIP-Silk Scaffolds Seeded with Primary Adipose

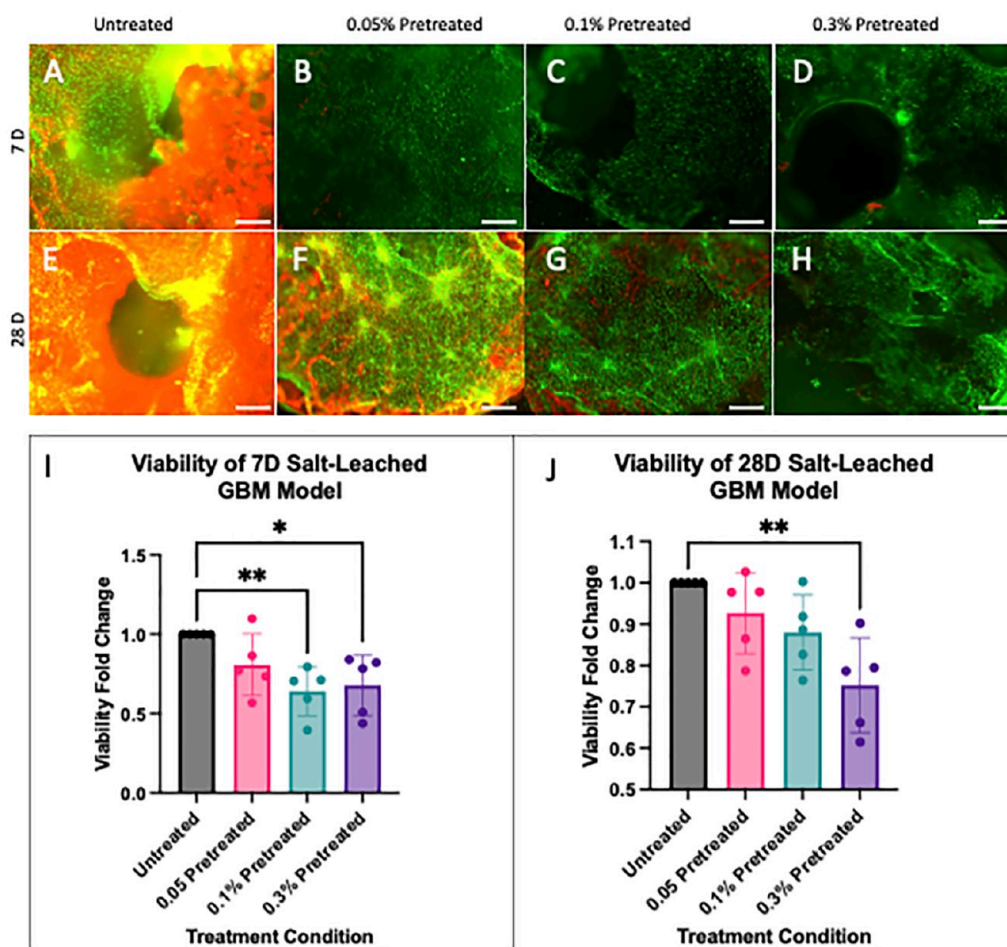


Figure 6. Live/Dead stain of 3D Brain-like tissue model salt-leached silk sponge+ECM. Green (Calcein AM) indicates live cells, and red (ethidium homodimer-1) indicates dead cells. A–D: Day 7 of culture. E–H: Day 28 of culture. Left to right: untreated, 0.05% SBB pretreated, 0.1% SBB pretreated, and 0.3% SBB pretreated. Scale bar = 500 μm . I, J: Viability of U87 GBM cells in salt-leached silk sponge+ECM system at 7 and 28 days in culture. Error bars represent standard deviation. Each distinct experiment contained 1–4 scaffold replicates, with 5 distinct experiments for each treatment condition ($N = 5$). The average of these scaffold replicates per experiment represents each dot (ANOVA with Dunnett's multiple comparison test, $*p = 0.033$, $**p \leq 0.0060$).

Tissue. HFIP-silk scaffolds are used to culture primary adipose tissue as a hypodermis layer for a full-thickness in vitro human skin model.¹⁸ 0.3% SBB postfixation treatment of the adipose scaffolds improved IF visualization compared to untreated scaffolds, but scaffold autofluorescence and background noise were still present. 0.1% SBB pretreated HFIP-silk scaffolds were seeded with adipose tissue and cultured 28 days. Immunofluorescence staining for vimentin was used to probe for fibroblasts as well as other mesenchymal cell types such as lymphocytes. The 0.1% SBB pretreatment reduced scaffold autofluorescence and improved resolution of cell markers compared to 0.3% SBB postfixation treatment (Figure 5). The survival of primary isolated cells over time in SBB pretreated HFIP-silk scaffolds confirmed the earlier findings that low concentrations of SBB pretreatment were suitable for cell culture on the HFIP-silk scaffolds.

Composite Systems: Salt-Leached Silk Scaffolds and ECM GBM Model. SBB Staining Successfully Quenched Autofluorescence in the GBM Tissue Model in Live Cell Imaging. With successful quenching of autofluorescence in the HFIP-silk scaffolds, similar trends were pursued in the silk-based ECM-containing 3D tissue model of glioblastoma.²⁰ In this tissue model, salt-leached donut-shaped silk sponges were

seeded with GBM cells, followed by the addition of a collagen-based hydrogel that both perfuses through the sponge and fills the inner window. This 3D brain-like ECM-containing system recapitulated ECM-dependent cellular responses in vitro associated with GBM phenotypes found in vivo.²⁰ The spatiotemporal responses of cells and the associated tumor microenvironments require high resolution imaging; thus, the SBB pretreatment was investigated.

Similar to the results with the HFIP-silk scaffolds, SBB pretreated salt-leached silk scaffolds seeded with U87-MG GBM cells demonstrated successful long-term suppression of autofluorescence at all concentrations of SBB. Untreated scaffolds showed high levels of autofluorescence, particularly in the red channel, at the same exposure levels as the pretreated conditions (Figure 6). Visually, there were fewer cells in the 0.3% SBB pretreatment condition after 7 days in culture when compared to the 0.05% and 0.1% pretreatment conditions, suggesting that higher concentrations of SBB negatively impact the cells, consistent with the results in the HFIP-silk scaffolds. After 28 days in culture, the GBM cell confluency recovered in the 0.1% SBB pretreated scaffolds. Only the 0.1% and the 0.05% SBB pretreated conditions supported tumor/spheroid formation. After 28 days of culture, the 0.05% and 0.1% SBB

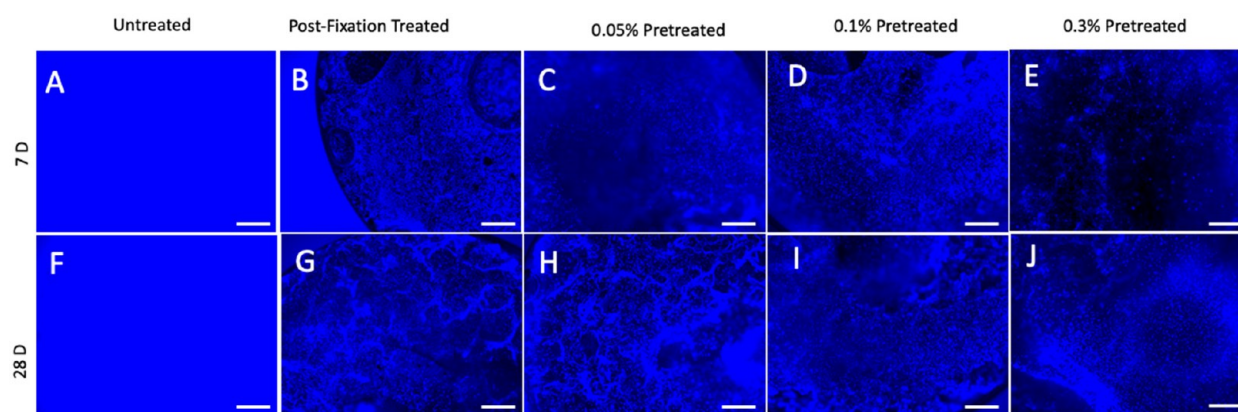


Figure 7. Immunofluorescence staining of U87 in a salt-leached silk sponge + ECM after 7 (A–E) and 28 (F–J) days of culture. Blue channel for DAPI 405 nm. Left to right: Untreated scaffold, 0.3% SBB postfixation treated, 0.05% SBB pretreated scaffold, 0.1% SBB pretreated scaffold, and 0.3% SBB pretreated scaffold. Scale bar = 500 μm .

pretreated scaffolds had diminished quenching capabilities in a concentration-dependent fashion, which was not seen in the 0.3% pretreatment. The cells were still easily visible at the lower concentrations after 28 days even with slight autofluorescence.

SBB Staining Did Not Significantly Affect Cell Viability at Lower Concentrations. The results from the live/dead staining were confirmed quantitatively through the WST-1 viability assay after 7 and 28 days. The untreated scaffolds supported significantly more viable cells than the 0.3% and 0.1% SBB pretreated scaffolds at day 7 ($p = 0.033$, $p = 0.006$, respectively). While the 0.05% SBB pretreated conditions demonstrated somewhat lower cell viability than that of the untreated control, the difference was not significant ($p = 0.164$), confirming the results of the live/dead stain (more spheroid formation in the 0.05% pretreated) (Figure 6). After 28 days of culture, the 0.3% SBB pretreated scaffolds had significantly lower cell viability than the untreated condition ($p = 0.0011$). The 0.1% SBB pretreated scaffolds recovered after 28 days and did not have a significantly lower cell viability than untreated scaffolds ($p = 0.1123$). The 0.05% SBB pretreated condition maintained similar results as the day 7 data ($p = 0.4358$). These results, along with live/dead imaging, indicated that 0.05% SBB pretreatment supported better viability than the other SBB pretreatment conditions, while successfully quenching the autofluorescence of the silk sponges.

Postfixation Treatment with SBB Was More Effective at Quenching Autofluorescence of the GBM Tissue Model Scaffolds than Pretreatment. SBB postfixation treatment successfully quenched autofluorescence of salt-leached silk scaffolds, but since the HFIP-silk scaffold SBB pretreatment showed improved immunofluorescence imaging, it was hypothesized that SBB pretreatment may quench autofluorescence and improve image resolution compared to postfixation SBB treatment of salt-leached sponges. SBB pretreatment would only be useful if it significantly improved imaging of the 3D GBM tissue model compared to postfixation SBB treatment due to the negative impact of SBB pretreatments on cell viability. A focus was placed on DAPI staining for the GBM tissue model to compare the ability of SBB pretreatments and postfixation treatment to quench silk autofluorescence during immunostaining because the blue channel (405 nm) typically results in high levels of autofluorescence (Figure 4).

The 0.3% postfixation SBB treated scaffolds had improved image quality and increased cell confluence than all the three other concentrations of SBB pretreated scaffolds, especially after 7 days (Figure 7). Image quality and cell confluency of the 0.05% SBB pretreated conditions were similar to SBB postfixation treated conditions after 28 days in culture. Higher concentrations of SBB pretreatment resulted in fewer cells and some silk autofluorescence (Figure 7).

In SBB pretreated GBM tissue models, only the salt-leached silk scaffold component was treated with SBB, and the collagen hydrogel added after cell seeding remained untreated. In GBM tissue models treated with SBB postfixation, the SBB stained both the silk sponge and the collagen hydrogel, likely leading to improved overall quenching of autofluorescence.

Composite Systems: Silk-Collagen Hydrogels. SBB postfixation treatment successfully quenched autofluorescence of silk-collagen hydrogels

Postfixation SBB treatment of silk-collagen gels was tested due to success of postfixation SBB treatment of the GBM tissue model with the collagen hydrogel component. Silk-collagen gels were stained with 0.3% SBB for 20 min following cell fixation but prior to cell permeabilization. Gels were stained for fibroblast marker vimentin (488 nm) as well as DAPI (405 nm). SBB postfixation treatment quenched autofluorescence and resulted in higher image resolution of the cells compared to untreated gels (SI Figure 2). SBB pretreatment of these silk-collagen gels was not feasible, since cells are incorporated into the gels during the matrix fabrication process. Postfixation SBB treatment successfully reduced autofluorescence for a clear visualization of cell morphology. Silk-collagen hydrogels provide another example of silk composite scaffolds that benefit from postfixation SBB treatment, much like the GBM tissue models.

Silk Hydrogels. SBB Postfixation Treatment Successfully Quenched Autofluorescence of Silk Hydrogels. SBB treatment using 2% and 4% silk hydrogels stained with 0.1% SBB for 20 min following cell fixation were used but prior to cell permeabilization due to the results from the GBM tissue model and silk-collagen hydrogels. Gels were stained with DAPI to visualize cell nuclei and a dramatic reduction of silk autofluorescence was found (SI Figure 3) compared to controls of cells cultured in untreated silk gels. There was no benefit to increasing the SBB concentration for the gels as concentrations below 0.1% w/v did not decrease autofluor-

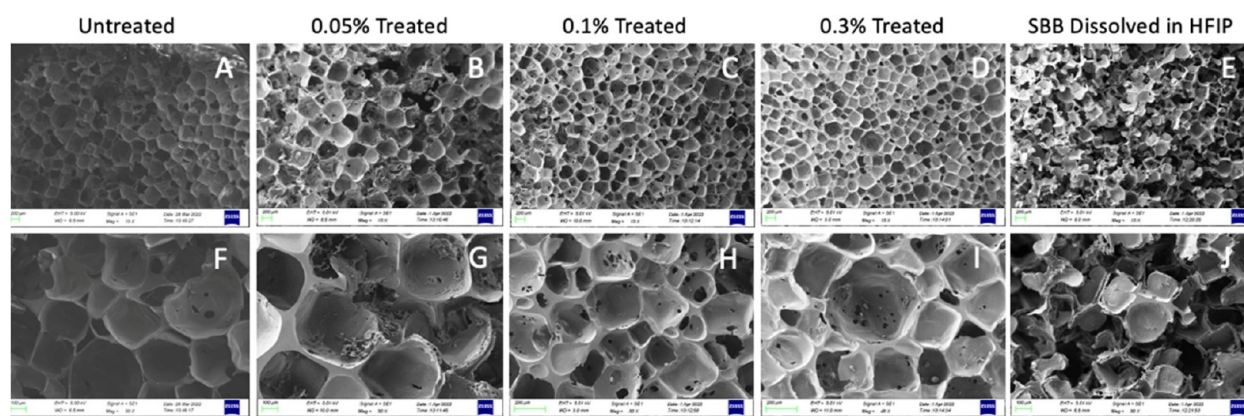


Figure 8. SEM images of various treatment conditions of the acellular HFIP-silk scaffolds. Left to right: untreated, 0.05% SBB treated, 0.1% SBB treated, 0.3% SBB treated, SBB dissolved in HFIP. A–E: 15× magnification. F–J: 49–50× magnification.

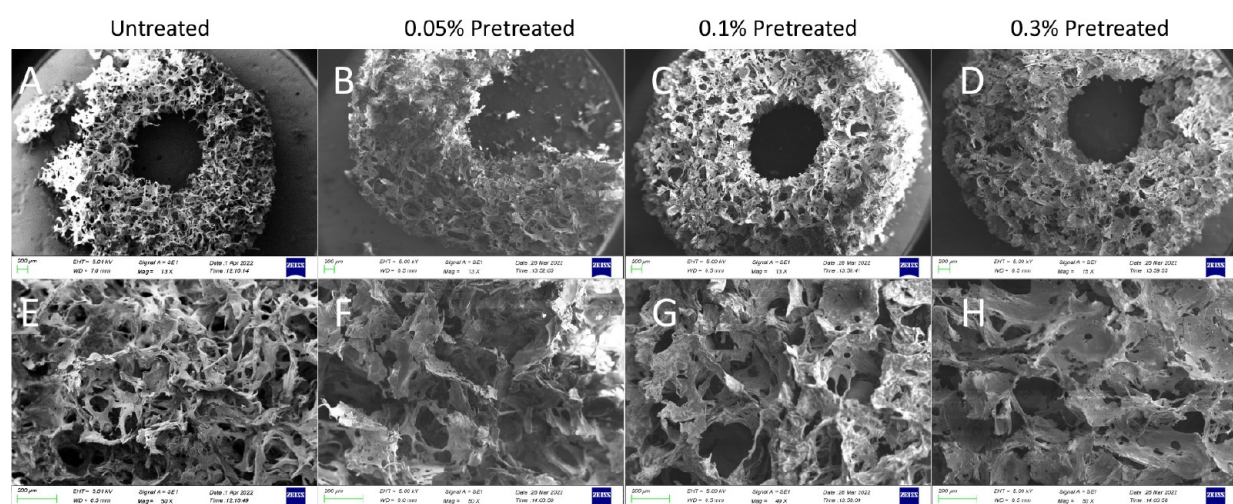


Figure 9. SEM Images of various treatment conditions of acellular salt-leached silk sponges for the GBM model. Left to right: untreated, 0.05% SBB treated, 0.1% SBB treated, and 0.3% SBB treated. A–D: 13–15× magnification. E–H: 50× magnification.

escence. Imaging of C2C12 cells cultured within 4% (SI Figure 4A, D) and 2% silk gels (SI Figure 4B, C, E, F) showed that SBB postfixation treatment reduced autofluorescence (SI Figure 4B, C). Additionally, SBB treatment did not interfere with cell membrane permeabilization for phalloidin (488 nm) to bind to and highlight cytoskeletal structure. The structures of growing and fusing muscle cells were visible in the SBB postfixation treated samples for C2C12 cells grown within 2% silk gels for 7 (SI Figure 4E) and 14 (SI Figure 4F) days. As all cells grown in hydrogels were fixed prior to imaging, the cell viability was not assessed for this SBB treatment. These results in combination with the results from the GBM tissue model and the silk-collagen hydrogels show that postfixation SBB treatment was effective at quenching autofluorescence for a variety of hydrogels and composite systems that incorporate silk, collagen, or a combination of these two materials.

Silk Gel-Spun Catheters. SBB Pretreatment and Postfixation Treatment Successfully Quenched Autofluorescence of Silk Gel-Spun Catheters. Both pretreatment and postfixation treatment of gel-spun silk catheters was completed on the basis of the results from the other formats of silk. Pretreatment of silk gel-spun catheters with SBB resulted in reductions in autofluorescence (SI Figure 5D–F), compared to nontreated catheters (SI Figure 5A–C). Cell attachment was not impaired by the catheter pretreatment (SI Figure 6). Both

pre- and post-treatment of catheters with SBB improved visualization of cell morphology and structure (SI Figure 5H - pretreated catheter) compared to non SBB-treated constructs (SI Figure 5G). Since no significant differences were found between pretreated and postfixation treated catheters, the staining can be carried out at any time for a given study.

Scaffold Characteristics. SBB Pretreatment Did Not Alter the Mechanical Properties of Silk-Based Systems but Coated Pores. Compression testing of the scaffolds demonstrated no significant differences between SBB treated and untreated scaffolds in terms of maximum stress or moduli at 7 and 28 days in culture for both the HFIP-silk scaffolds and the GBM tissue model scaffolds (SI Figures 7 and 8). Tensile testing of the silk gel-spun catheter systems also showed no significant differences between treated and untreated catheters (SI Figure 5).

Scanning electron microscopy revealed that SBB pretreatment on the scaffolds did not affect the scaffold shape and pore structure at all concentrations of SBB pretreatment, except in HFIP-silk scaffolds that were prepared using SBB dissolved in HFIP during scaffold fabrication (Figure 8). A coating/smoothing effect was observed on the pores of the SBB treated scaffolds, and increased SBB pretreatment concentration increased pore occlusion. Pore size and spacing remained regular for the pretreated conditions compared to those of

Table 1. Summary of Results from SBB Postfixation Treatment and Pretreatment Comparisons among the Silk Protein-Based Biomaterials Tested

Model System	SBB Pretreatment	SBB Post-Fixation Treatment
HFIP-Silk Scaffolds with Human Fibroblasts	0.1% SBB pretreatment showed best autofluorescence quenching for live cell and postfixation imaging	0.3% SBB postfixation treatment showed adequate autofluorescence quenching for postfixation imaging
HFIP-Silk Scaffolds with Human Adipose Tissue	0.1% SBB pretreatment showed best autofluorescence quenching for live cell and postfixation imaging	0.3% SBB postfixation treatment showed adequate autofluorescence quenching for postfixation imaging
Salt-Leached Silk Sponge GBM Model	0.05% SBB pretreatment showed adequate autofluorescence quenching for live cell imaging, but seems to disturb collagen gel adhesion to the silk sponge	0.3% SBB postfixation treatment showed best autofluorescence quenching for post-fixation imaging, and is recommended over live-cell imaging
Gel Spun Silk Catheters with C2C12 Cells	0.1% SBB pretreatment showed equivalent autofluorescence quenching to postfixation treatment for postfixation imaging	0.3% SBB postfixation treatment showed equivalent autofluorescence quenching to pretreatment for postfixation imaging
Silk-Collagen Hydrogels with Human Fibroblasts	SBB pretreatment not compatible with hydrogel fabrication	0.3% SBB postfixation treatment showed best autofluorescence quenching for post-fixation imaging
Silk Hydrogels with C2C12 Cells	SBB pretreatment not compatible with hydrogel fabrication	0.3% SBB postfixation treatment showed best autofluorescence quenching for post-fixation imaging

untreated scaffolds for both the HFIP-silk scaffolds (Figure 8) and the GBM tissue model scaffolds (Figure 9). SBB dissolved in HFIP during scaffold fabrication caused irregular pore size, which may impact cell attachment and growth.

DISCUSSION

SBB Pretreatment Quenched Autofluorescence of Silk-Based Matrices. SBB pretreatment was tested at multiple concentrations on various silk and silk-composite scaffolds and cell types to determine optimal concentrations for maximal suppression of silk autofluorescence and the minimum impact on the cell viability and fluorescence images. The 0.05%, 0.1%, and 0.3% (w/v) SBB pretreatments were tested on HFIP-silk scaffolds seeded with human dermal fibroblasts and on salt-leached scaffolds seeded with human U87-MG GBM cells. For both systems, image contrast increased, and scaffold autofluorescence decreased with increasing SBB concentration. NHDF cells in HFIP-silk scaffolds pretreated with 0.3% SBB presented rounded morphology and lower confluence than other test conditions, while 0.05% and 0.1% SBB pretreated scaffolds supported improved cell viability compared to the 0.3% pretreated. GBM cells in salt-leached scaffolds formed spheroids in the 0.1% and 0.05% SBB pretreated conditions, indicating that lower treatment concentrations were better suited to support normal cell growth and behavior.

The correlation between higher SBB concentration and lower cell viability could be explained by both increasing concentrations of SBB leaching from the scaffolds, which can be cytotoxic to the cells, and the SBB pretreatments producing a coating on the scaffolds, which may interfere with initial cell attachment as indicated by the SEM images (Figure 8 and Figure 9). This reduced cell attachment area did not affect overall cell proliferation or growth over long-term culture. The decreased cell viability in pretreated scaffolds (HFIP-silk and salt-leached) at day 7 that recovered by day 28 (compared to untreated scaffolds) suggests that short-term experiments may be impacted by the SBB stain, and thus a different quenching method or postfixation staining may be preferable for shorter time points. This could be overcome by seeding scaffolds at a higher cell density if a certain cell count within the scaffolds is desired. Another consideration for the 3D GBM tissue model was that collagen hydrogel perfusion was more effective through the untreated scaffolds compared to the SBB pretreated scaffolds. In the SBB pretreated scaffolds, the hydrogel often remained on the top of the scaffold and only in

the middle window, rather than penetrating through the entire scaffold as it does in untreated conditions. This can also be explained via the SEM images, where the pores are filled in with the SBB coating (Figure 8 and Figure 9), reducing collagen infiltration. Despite the changes to the surface morphology and the impact on collagen gel adhesion to the sponge scaffold, mechanical analysis showed no statistically significant changes to the Young's modulus or maximum compressive stress of the treated and untreated scaffolds, indicating that the SBB treatment did not affect mechanical properties of the scaffolds (SI Figures 7 and 8). Since SBB interacts with the hydrophobic regions of silk, it was hypothesized that the salt-leached scaffolds, which contain higher degrees of crystallinity (β sheet content) than the HFIP-silk scaffolds, would result in lower concentrations of SBB required to stain the GBM tissue model scaffolds. However, FT-IR results (SI Figure 9) indicated that there were no significant differences between the β sheet content. The difference in optimal concentration may be attributed to the increased interconnectivity between the pores of the salt-leached scaffolds compared to the HFIP-silk scaffolds (Figure 8 and Figure 9), leading to a better perfusion of SBB solution throughout the salt-leached scaffolds. Concentrations of SBB as low as 0.05% improved the ability to visualize cells via live/dead staining due to the decreased autofluorescence of the scaffold, with improved contrast as SBB concentration increased. These findings highlight the value of SBB treatment for cell imaging studies using silk scaffolds, with minimal undesirable impact on other scaffold attributes.

For HFIP-silk scaffolds, 0.1% SBB pretreatment was the optimal treatment concentration due to its ability to suppress autofluorescence, increase image contrast, and maintain normal cell morphology and proliferation. The culture of primary adipose tissue on 0.1% SBB pretreated HFIP-silk scaffolds further confirmed that this pretreatment provided the suppression of autofluorescence for improved imaging of primary cell types on the scaffolds. In contrast, for the 3D GBM tissue model, the SBB pretreatment should be utilized for live cell imaging exclusively, as the postfixation SBB treatment seems appropriate for fixed staining methods. For live cell imaging, the optimal SBB concentration for the 3D GBM tissue model that demonstrated improved cell viability while quenching autofluorescence was 0.05% SBB. There were no significant differences between 0.05% pretreated and untreated scaffolds in terms of viability and live/dead images, confirming successful long-term quenching of autofluorescence

cence. Postfixation SBB treated scaffolds displayed similar levels of autofluorescence suppression as the SBB pretreated scaffolds in fixed-staining applications. Postfixation SBB treatment avoided decreased cell viability associated with SBB pretreatment at higher concentrations. Additionally, as the postfixation SBB treatment was a less time-consuming process, pretreatment may only be valuable for studies where live cell imaging is preferable, such as in drug delivery trials for this 3D GBM tissue model or for cell tracking studies.

Postfixation SBB treatment of the silk-collagen hydrogels with NHDFs and silk hydrogels with myoblasts present other examples of silk-based biomaterials that benefit from postfixation SBB treatment. Gel-spun silk catheters present an example of a scaffold that benefits equally from both pretreatment and postfixation SBB treatment, allowing for options depending on the experimental needs. Table 1 summarizes the results of pretreatment and postfixation treatment comparison among model systems utilized in this manuscript.

This study demonstrated that SBB pretreatment can be useful for quenching autofluorescence of various silk-based biomaterials, and optimization of SBB pretreatment concentrations should be considered for each intended application.

■ SIGNIFICANCE OF PRETREATMENT

While the use of SBB to quench silk autofluorescence is not novel, this work provides standardized, reproducible, and reliable methods. This approach also has not been previously used during silk material fabrication to generate constructs that are pretreated to reduce autofluorescence. The range of applications encompassing many scaffold and cell types provides new and broadened insight into the use of SBB in many areas of silk biomaterials applications.

Previously, the efficacy of SBB staining to suppress autofluorescence of silk scaffolds was addressed by comparing SBB treatment either immediately after fixation of cells or as the last step of immunofluorescence staining protocol.¹⁴ In both methods, SBB effectively quenched endogenous fluorescence of silk biomaterials while maintaining a good image resolution of cells and proteins fluorescently tagged on the scaffolds. Treatment with SBB postfixation prior to immunostaining better maintained fluorescent tagging and suppressed autofluorescence compared to incubating SBB with scaffolds after completing the immunostaining protocol, indicating that the choice of when to treat with SBB can impact the effectiveness of this treatment.¹⁴ For silk scaffolds, SBB has only been applied as a postfixation treatment since it is typically solubilized in 70% ethanol, which is toxic to cells.

Postfixation treatment options do not offer a method to obtain live cell fluorescent images, which is a widely used method to evaluate cell viability in culture. SBB pretreatment of silk scaffolds provides an effective method for suppressing autofluorescence for live cell imaging. Live/dead staining and imaging are possible in 3D silk scaffolds that are pretreated with at least 0.05% SBB solution. SBB pretreatment also proved more effective at decreasing the autofluorescence of silk than postfixation SBB treatment for some applications, increasing the image contrast. Having several methods that can be selected on the basis of the scaffold type allows for improved analysis of cell morphology and distribution within 3D silk scaffolds. Other hydrophobic polymers that experience autofluorescence may also be stainable via these methods. Ultimately, this study provides a roadmap for utilizing SBB as a

quenching stain to improve cell imaging in 3D biomaterial constructs.

■ ASSOCIATED CONTENT

Supporting Information

The Supporting Information is available free of charge at <https://pubs.acs.org/doi/10.1021/acsbmaterials.3c00145>.

Contains stress/strain data of the scaffolds, immunofluorescence staining of C2C12 cells in silk hydrogels systems and catheter systems, immunofluorescence staining of NHDF in HFIP-silk scaffolds after 7 days of culture, as well as FT-IR data (PDF)

■ AUTHOR INFORMATION

Corresponding Author

David L. Kaplan – Department of Biomedical Engineering, Tufts University, Medford, Massachusetts 02155, United States; orcid.org/0000-0002-9245-7774; Email: david.kaplan@tufts.edu

Authors

Olivia Foster – Department of Biomedical Engineering, Tufts University, Medford, Massachusetts 02155, United States

Sawnaz Shaidani – Department of Biomedical Engineering, Tufts University, Medford, Massachusetts 02155, United States

Sophia K. Theodossiou – Department of Biomedical Engineering, Tufts University, Medford, Massachusetts 02155, United States

Thomas Falcucci – Department of Biomedical Engineering, Tufts University, Medford, Massachusetts 02155, United States

Derek Hiscox – Department of Biomedical Engineering, Tufts University, Medford, Massachusetts 02155, United States

Brooke M. Smiley – Department of Biomedical Engineering, Tufts University, Medford, Massachusetts 02155, United States

Chiara Romano – Department of Biomedical Engineering, Tufts University, Medford, Massachusetts 02155, United States

Complete contact information is available at:

<https://pubs.acs.org/doi/10.1021/acsbmaterials.3c00145>

Author Contributions

[†](O.F., S.S., S.K.T.) These authors contributed equally.

Notes

The authors declare no competing financial interest.

■ ACKNOWLEDGMENTS

We would like to thank Dr. Onur Hasturk and Dr. Emily Hartzell for their help with statistics and deconvolution; Dr. Junqi Wu for her help with SEM; Edward Gordon for suggesting SBB for postfixation which led to this study; and undergraduatesCarolynn Brooks, Madison Fletcher, and William Friedman for their assistance with assays. We thank the NIH (P41EB027062, T32EB016652-01A1, 5K12GM133314-02), the AFOSR (FA9550-20-1-0363) and the ARO (W911NF2120130) for support for this study.

■ REFERENCES

(1) Singh, M. R.; Patel, S.; Singh, D. Chapter 9 - Natural polymer-based hydrogels as scaffolds for tissue engineering. In *Nano-*

biomaterials in Soft Tissue Engineering; Grumezescu, A. M., Ed.; William Andrew Publishing, 2016; pp 231–60.

(2) Qi, L.; Knapton, E. K.; Zhang, X.; Zhang, T.; Gu, C.; Zhao, Y. Pre-culture Sudan Black B treatment suppresses autofluorescence signals emitted from polymer tissue scaffolds. *Sci. Rep.* **2017**, *7* (1), 8361.

(3) Amirikia, M.; Shariatzadeh, S. M. A.; Jorsaraei, S. G. A.; Mehranjani, M. S. Auto-fluorescence of a silk fibroin-based scaffold and its interference with fluorophores in labeled cells. *Eur. Biophys. J.* **2018**, *47* (5), 573–81.

(4) Viegas, M. S.; Martins, T. C.; Seco, F.; do Carmo, A. An improved and cost-effective methodology for the reduction of autofluorescence in direct immunofluorescence studies on formalin-fixed paraffin-embedded tissues. *Eur. J. Histochem.* **2007**, *51* (1), 59–66.

(5) Oliveira, V. C.; Carrara, R. C.; Simoes, D. L.; Saggioro, F. P.; Carlotti, C. G., Jr.; Covas, D. T.; Neder, L. Sudan Black B treatment reduces autofluorescence and improves resolution of in situ hybridization specific fluorescent signals of brain sections. *Histol Histopathol* **2010**, *25* (8), 1017–1024.

(6) Baschong, W.; Suetterlin, R.; Laeng, R. H. Control of autofluorescence of archival formaldehyde-fixed, paraffin-embedded tissue in confocal laser scanning microscopy (CLSM). *J. Histochem Cytochem* **2001**, *49* (12), 1565–72.

(7) Schnell, S. A.; Staines, W. A.; Wessendorf, M. W. Reduction of lipofuscin-like autofluorescence in fluorescently labeled tissue. *J. Histochem Cytochem.* **1999**, *47* (6), 719–30.

(8) Romijn, H. J.; van Uum, J. F.; Breedijk, I.; Emmering, J.; Radu, I.; Pool, C. W. Double immunolabeling of neuropeptides in the human hypothalamus as analyzed by confocal laser scanning fluorescence microscopy. *J. Histochem Cytochem.* **1999**, *47* (2), 229–36.

(9) Erben, T.; Ossig, R.; Naim, H. Y.; Schnekenburger, J. What to do with high autofluorescence background in pancreatic tissues - an efficient Sudan black B quenching method for specific immunofluorescence labelling. *Histopathology.* **2016**, *69* (3), 406–22.

(10) Jaafar, I. H.; LeBlon, C. E.; Wei, M. T.; Ou-Yang, D.; Coulter, J. P.; Jedlicka, S. S. Improving fluorescence imaging of biological cells on biomedical polymers. *Acta Biomater.* **2011**, *7* (4), 1588–98.

(11) Chwalek, K.; Tang-Schomer, M. D.; Omenetto, F. G.; Kaplan, D. L. In vitro bioengineered model of cortical brain tissue. *Nat. Protoc.* **2015**, *10* (9), 1362–73.

(12) Chen, Y.; Lin, Y.; Davis, K. M.; Wang, Q.; Rnjak-Kovacina, J.; Li, C.; Isberg, R. R.; Kumamoto, C. A.; Meccas, J.; Kaplan, D. L. Robust bioengineered 3D functional human intestinal epithelium. *Sci. Rep.* **2015**, *5*, 13708.

(13) Bellas, E.; Seiberg, M.; Garlick, J.; Kaplan, D. L. In vitro 3D full-thickness skin-equivalent tissue model using silk and collagen biomaterials. *Macromol. Biosci.* **2012**, *12* (12), 1627–36.

(14) Neo, P. Y.; Tan, D. J.; Shi, P.; Toh, S. L.; Goh, J. C. Enhancing analysis of cells and proteins by fluorescence imaging on silk-based biomaterials: modulating the autofluorescence of silk. *Tissue Eng. Part C Methods* **2015**, *21* (2), 218–28.

(15) Hasturk, O.; Jordan, K. E.; Choi, J.; Kaplan, D. L. Enzymatically crosslinked silk and silk-gelatin hydrogels with tunable gelation kinetics, mechanical properties and bioactivity for cell culture and encapsulation. *Biomaterials* **2020**, *232*, 119720.

(16) Fonovich, T. M. Sudan dyes: are they dangerous for human health? *Drug and Chemical Toxicology.* **2013**, *36* (3), 343–52.

(17) Pritchard, E. M.; Hu, X.; Finley, V.; Kuo, C. K.; Kaplan, D. L. Effect of silk protein processing on drug delivery from silk films. *Macromol. Biosci.* **2013**, *13* (3), 311–20.

(18) Vidal, S. E. L.; Tamamoto, K. A.; Nguyen, H.; Abbott, R. D.; Cairns, D. M.; Kaplan, D. L. 3D biomaterial matrix to support long term, full thickness, immuno-competent human skin equivalents with nervous system components. *Biomaterials* **2019**, *198*, 194–203.

(19) Rockwood, D. N.; Preda, R. C.; Yücel, T.; Wang, X.; Lovett, M. L.; Kaplan, D. L. Materials fabrication from Bombyx mori silk fibroin. *Nat. Protoc.* **2011**, *6* (10), 1612–31.

(20) Sood, D.; Tang-Schomer, M.; Pouli, D.; Mizzoni, C.; Raia, N.; Tai, A.; Arkun, K.; Wu, J.; Black, L. D.; Scheffler, B.; Georgakoudi, I.; Steindler, D. A.; Kaplan, D. L. 3D extracellular matrix microenvironment in bioengineered tissue models of primary pediatric and adult brain tumors. *Nature Communications.* **2019**, *10* (1), 4529.

(21) Vidal Yucha, S. E.; Tamamoto, K. A.; Nguyen, H.; Cairns, D. M.; Kaplan, D. L. Human Skin Equivalents Demonstrate Need for Neuro-Immuno-Cutaneous System. *Adv. Biosyst.* **2019**, *3* (1), No. 1800283.

(22) Lovett, M. L.; Cannizzaro, C. M.; Vunjak-Novakovic, G.; Kaplan, D. L. Gel spinning of silk tubes for tissue engineering. *Biomaterials* **2008**, *29* (35), 4650–7.

(23) Sood, D.; Tang-Schomer, M.; Pouli, D.; Mizzoni, C.; Raia, N.; Tai, A.; Arkun, K.; Wu, J.; Black, L. D., 3rd; Scheffler, B.; Georgakoudi, I.; Steindler, D. A.; Kaplan, D. L. 3D extracellular matrix microenvironment in bioengineered tissue models of primary pediatric and adult brain tumors. *Nat. Commun.* **2019**, *10* (1), 4529.

(24) Xiang, N.; Yuen, J. S. K.; Stout, A. J.; Rubio, N. R.; Chen, Y.; Kaplan, D. L. 3D porous scaffolds from wheat glutenin for cultured meat applications. *Biomaterials.* **2022**, *285*, 121543.